World Academy of Science, Engineering and Technology
International Journal of Mechanical and Materials Engineering
Vol:15, No:2, 2021

Deformation and Crystallization in a 7075-T651 Friction Stir Weld

C. S. Paglia

***Abstract*—**The deformation and the crystallization in a 7075-T651 friction stir weld, in particular for regions directly in contact with the mechanical action of the rotating probe, have been investigated by means of optical microscopy. The investigation enabled to identify regions of the weld differently affected by the deformation caused by the welding process. The highly deformed grains in the horizontal direction close to the plate margin were indicative of shear movements along the horizontal plane, while highly deformed grains along the plate margin in the vertical direction were indicative of vertical shear movements of opposite directions, which superimposed the shear movement along the horizontal plane. The vertical shear movements were not homogeneous through the plate thickness. The microstructure indicated that after the probe passes, the grain growth may take place under static conditions. The small grains microstructure of the nugget region, formed after the main dynamic recrystallization process, develops to an equiaxed microstructure. A material transport influenced by the rotating shoulder was also observed from the trailing to the advancing side of the weld.

***Keywords*—**AA7075-T651, friction stir welding, deformation, crystallization.

I. Introduction

FRICTION stir welding (FSW) is a solid state welding process that was developed by The Welding Institute (TWI) in 1991 [1]. The joining process consists of a rotating tool which plastically deforms the material along the joining line [1]. The weld tool is composed of a shoulder and a protrusion called probe. The movement of the shoulder and the probe generates material flow and heat [2]. The rotating tool forms a highly deformed plastic zone, which dynamically recrystallizes due to the frictional heat and the shear strain [3]. Several thermal models indicated that melting is not occurring during FSW [4], [5]. Although two main heat sources are present during FSW, the friction heat input generated near the probe appears to be the main source [5]. A numerical and experimental simulation of the heat transfer process has also been performed during the tool penetrating and removing period [6], while a thermo-mechanical model describes the thermal history, stress distribution and mechanical forces in the longitudinal, lateral and vertical directions, which appear to be largely influenced by the welding parameters [7]. A heat transfer model, in particular for the penetrating and pulling up processes, was also presented [6]. An increase in temperature with the depth was observed as the tool penetrates the workpiece. The temperature distribution during the main weld process does not change significantly, so that the heat transfer is assumed a quasi-steady state one. After the pull out process, the temperature of the workpiece gradually decreases [6]. Since melting of material is not reached during this joining process [8], a lowered incidence of weld defects and residual stresses is achieved.

The flow visualization and residual microstructures associated with FSW have been recently investigated by welding dissimilar materials [2], [9], or by using a marker technique [10]. The flow pattern generally observed varies from complex spirals and vortex-like structures [10] to a non-symmetrical material transport about the weld center line, where the material is transported behind its original position. A motion of material along the horizontal plan is superimposed by a circulation of material about the longitudinal weld axis [10]. The evolution of the microstructure during FSW has also been recently investigated with a friction stir processing technique, where the process is limited to a single-work piece with no welding [11]. It was found that, the microstructure evolution during FSW/FSP undergoes various mechanisms such as discontinuos-continuous dynamic recrystallization, grain growth, dislocation introduction, dynamic recovery. Consequently the evolution of individual grains may be different [11].

The aim of the present work is to investigate the deformation and the crystallization occurring during FSW by observing the different microstructural features in particular for regions directly in contact with the rotating probe.

II. Experimental Procedure

Aluminum 7075-T651 plates (300 x 100 x 10 mm) were friction stir welded at a travel speed of 140 mm/min and with a rotation speed of 240 rpm. The shoulder was 7° inclined concave and had a diameter of 2.85 cm. The pin had a diameter of 10 mm with a cylindrical shape and a length of 0.95 cm. The welding process was developed under force control and the controlled Z force was 6123 kg. The welding direction was parallel to the rolling direction and the final weld was 260 mm long.

The weld zones such as the heat affected zones (HAZ), the highly deformed zones adjacent to the weld nugget; i.e., the thermo-mechanically affected zones (TMAZ) and the weld nugget are schematically shown in Fig. 1. The parent metal represents the unaffected region of the weld.

The microstructure was investigated with an optical microscope by polishing the surface (1 μm) and etching with Keller's reagent.

C. S. Paglia is with the University of Applied Sciences of Southern Switzerland, DACD, Trevano, CP 12, 6952 Canobbio, Switzerland (phone: +41 (0)58 666 63 61; fax +41 (0)58 666 63 59; e-mail: christian.paglia@supsi.ch).

Open Science Index, Mechanical and Materials Engineering Vol:15, No:2, 2021 publications.waset.org/10011823.pdf

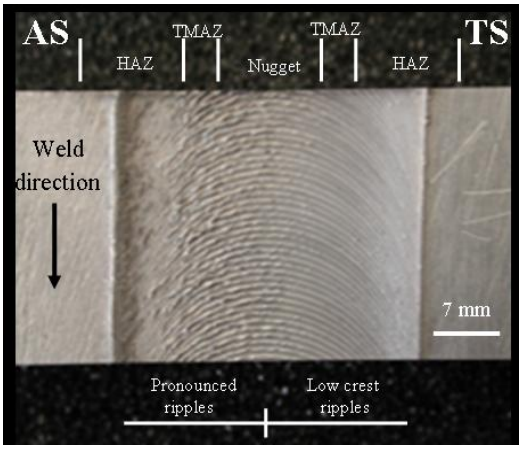

Fig. 1 Surface morphology of the friction stir weld. Note the slight material transport caused by the rotation of the tool shoulder from the trailing side (TS) to the advancing side (AS). Weld zones: TMAZ and HAZ

III. Results

A top view of the weld track produced by the shoulder movement indicates pronounced surface ripples and a more prominent edge towards the AS of the weld as compared to the TS (Fig. 1). A microstructural overview of the weld cross section in the steady-state condition and in the final weld region, where the probe is extracted, is depicted in Fig. 2. Interestingly, the shape of the nugget for the steady-state welding condition is slight asymmetrical as compared to the nugget in the final weld region (Fig. 2).

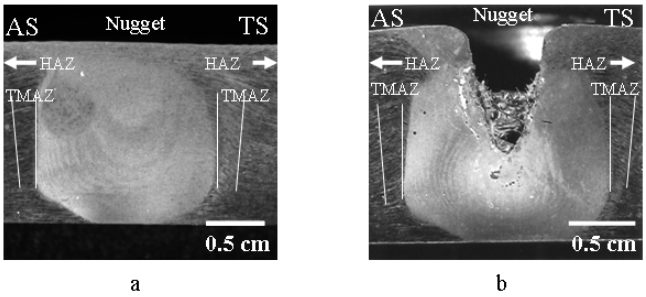

Fig. 2 Micrographs of the weld cross section (a) and of the region where the rotating pin is extracted (b). The different weld zones are schematically represented

A closer investigation of the initial weld section, where the plate margin is still clearly recognizable (Fig. 3) indicates a band-like structure formed by the grains near the plates margin (Fig. 3 (a)). Towards the top of the weld cross section a slight shear is detected along the plate margins (Fig. 3 (b)). Approximately 1 cm away from the plate margin, an elongated grain structure is present and the grain boundaries are more clearly recognizable (Fig. 3 (c)) as compared to the regions located along the plate margin, where a band-like structure is dominant (Figs. 3 (a), (b)).

Close the plate margin, small grains are alternated by the banded structure (Fig. 4).

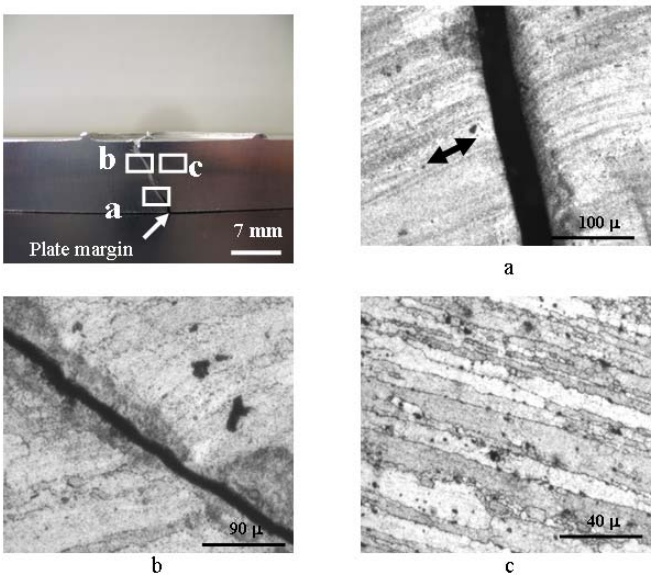

Fig. 3 Deformation along the plates margin (partial penetration of the tool), a: highly deformed grains, b: vertical shear, c: elongated grains away from the plates margin. The pictures are located in the plunge area of the welding tool. In the initial area of the weld, the plate margin is still recognizable and the pictures were taken 0.5 cm below the plate surface

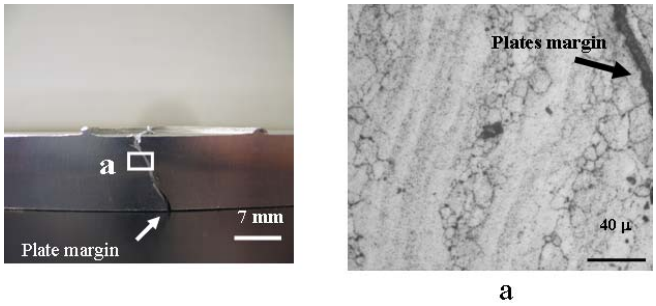

Fig. 4 Crystallization near the plates margin: banded structure and fine equiaxed grains (detail of Fig. 3)

As we move away from the initial weld region, a narrow shear zone with highly deformed grains along the plates margin is still clearly visible (Fig. 5 (a)). From the plate margin toward the weld center line, the elongated and deformed grains decrease, while gradually a finer equiaxed structure recrystallizes (Figs. 5 (b)-(d)).

Along the weld center line, where the small equiaxed microstructure of the nugget starts to recrystallize, horizontal bands at the bottom and at the top of the weld are present (Figs. 6 (a), (b)). For the steady-state condition, the nugget clearly exhibits a sharp boundary with the TMAZ in the AS, while a more diffuse boundary is observed in the TS (Fig. 6). At this stage folds characterize the TS of the nugget (Fig. 6 (c)), while plastic deformation bands in form of rings are mainly recognizable in the AS of the nugget (Fig. 6 (d)).

The plastic deformation bands become wider toward the center of the nugget. In the flow arm region, small grains are visible (Fig. 7).

Open Science Index, Mechanical and Materials Engineering Vol:15, No:2, 2021 publications.waset.org/10011823.pdf

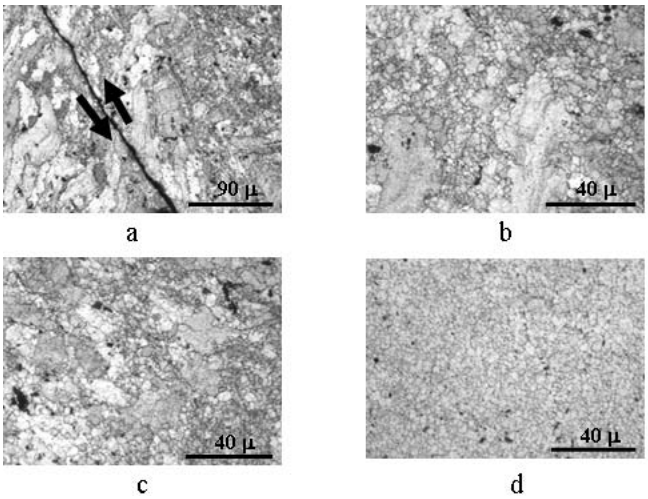

Fig. 5 Deformation and crystallization close (a) and away (d) from the plate margin weld line. (a) vertical shear along the plates margin, (b) elongated and small grains, (c) coarse equiaxed and fine grains, (d) fine equiaxed grains. The pictures are located in the plunge area of the welding tool in a region where the heat produced by the welding tool causes the recrystallization of the elongated grains. The plate margin is still recognizable and the pictures were taken 0.5 cm below the plate surface

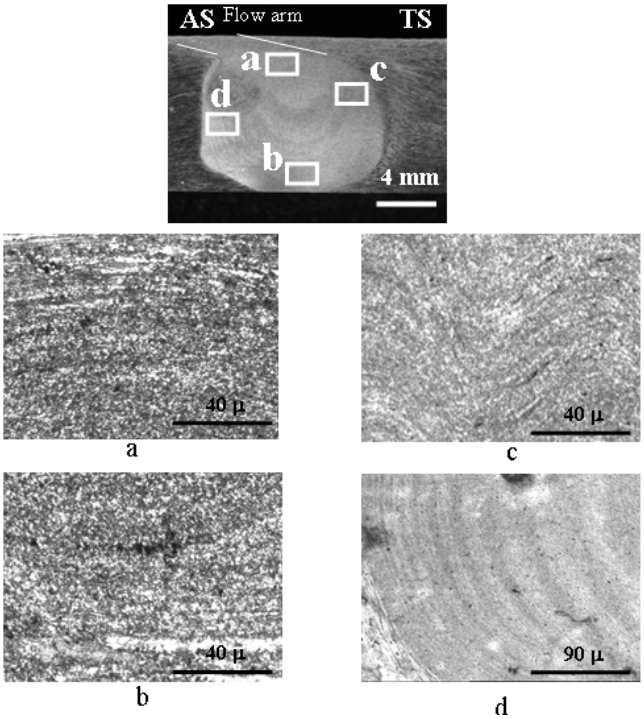

Fig. 6 Microstructure in the nugget weld zone: (a), (b) Horizontal bands of fine equiaxed grains, (c) Folded microstructure in the TS of the nugget, (d) Concentric ring microstructure. Note the widening of the bands towards the center of the nugget

The final weld region exhibits highly deformed grains parallel to the horizontal plane within a layer close to the rotational zone (Fig. 8 (a)). A microstructure with small grains is observed away from the rotational zone on a layer in the vertical plane 0.5 mm closer to the reader (Fig. 8 (b)). A top view of the final weld region indicates a slight increase in the grain diameter by approaching the rotational zone (Figs. 8 (c), (d)) in the TS of the weld.

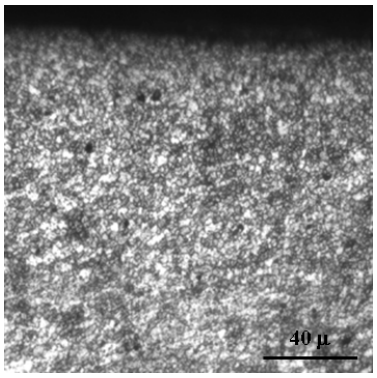

Fig. 7 Microstructure with small grains in the flow arm region

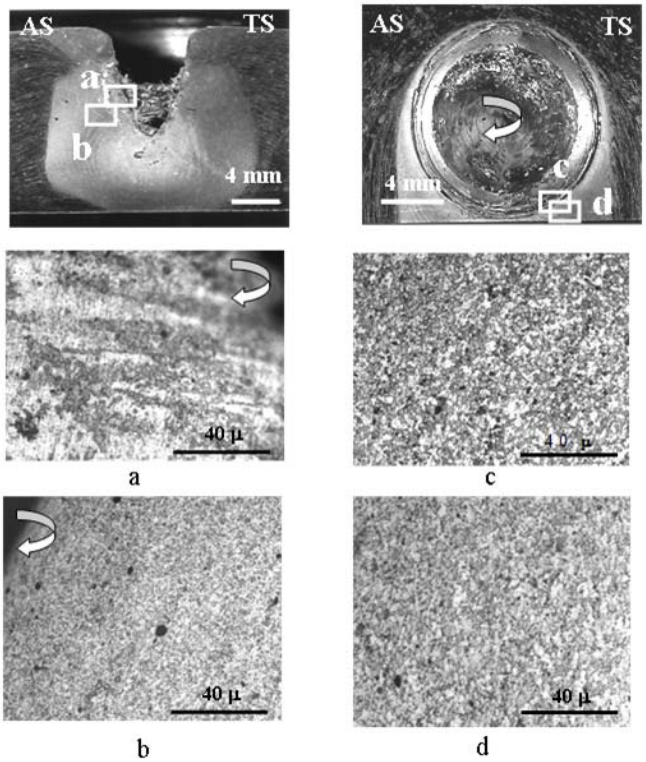

Fig. 8 Microstructure in the final weld region. The region b represents a layer in the vertical plane, 0.5 mm closer to the reader

It is interesting to note that the grains present in the TS of the weld, close to the rotational zone, are generally small, but not really equiaxed as observed in particular for the weld nugget in the steady-state welding condition.

IV. Discussion

The microstructural investigation provides interesting information on the deformation-crystallization processes taking place during FSW, although no metal flow studies [9], [10], [12] have been carried out in this work. As observed in other works [10], [13], a material transport caused by the

Open Science Index, Mechanical and Materials Engineering Vol:15, No:2, 2021 publications.waset.org/10011823.pdf

Open Science Index, Mechanical and Materials Engineering Vol:15, No:2, 2021 publications.waset.org/10011823.pdf

shoulder movement is taking place from the trailing to the AS of the weld (Fig. 1). In regions only slightly affected by the rotating probe, the plate margin is still well recognizable and the recrystallization process has only partially started. In these regions the deformation taking place on the backside of the rotating probe can be recognized (Figs. 3 (a), (b)). These regions, in fact, allow to identify two main components of the movement occurring during the FSW, a horizontal component identified by the highly elongated banded structures along the plate margin (Fig. 3 (a)), and a superimposed vertical component indicated by the vertical shear along the plate margin (Fig. 3 (b)). A translation motion along the horizontal plane as well as a vertical motion was also observed in material flow studies by using tracer techniques [12] or by welding dissimilar materials [13]. In regions where the plate margin is still recognizable, the extent of the deformation and the temperature are not yet high enough to cause recrystallization, even though small round grains start to form between the highly deformed banded structure along the plate margin (Fig. 4). Regions of the weld mechanically affected by the rotating action of the probe, exhibit a more clear deformation and crystallization (Fig. 5). Here, a vertical deformation with opposite directions is present within a very narrow region, for instance 90 μ, and is confirmed by an increased shear and grain distortion along the plates margin (Fig. 5 (b)). Within the nugget, horizontal deformation bands are observed at the top and at the bottom edges (Figs. 6 (a), (b)). The vertical plastic deformation, therefore, is apparently not homogeneous throughout the vertical plate thickness and appears to be influenced by the shoulder movement in the upper part of the weld during steady-state welding conditions [12]. In the lower part of the nugget, the viscoplastic material flow appears to be largely affected by the presence of the backing plate, which forces all the deformation to occur within a narrow die volume. Within weld regions highly affected by the rotating probe and by the high temperature, the extent of the deformation appears to be generally high (Fig. 5). A deformation gradient exists from the distorted plate margin, toward the weld center line. Here, a recrystallized microstructure with small grains is present. From the plate margin toward the weld center line, the grains start a dynamic recrystallization process becoming smaller and more equiaxed in the center of the weld (Figs. 5 (a), (d)). The stirring action of the rotating probe deforms the material until the stored energy reaches a level to promote dynamic recrystallization [9]. The recrystallized grains are smaller in diameter as the original subgrain size and the presence of dislocation tangles at grain boundaries, OIM measurements [14], as well as a comparison with microstructures formed via hot forging or torsion [18] indicate the dynamic recrystallization to take place as a continuous process. Away from the weld center line the grains are highly deformed. Towards the weld center line, the original deformed and elongated grain microstructure is superimposed by the recrystallization process and becomes less apparent. Within the nugget weld zone of the steady-state welding region, however, deformation features such as bands and folds are still present. Interestingly, plastic deformation bands are more clearly present towards the AS (Fig. 6 (d)), while folds are present in the TS (Fig. 6 (c)). This confirms a general asymmetrical material flow around the probe [10], [12]. In the AS, the shear stress of the probe surface is superimposed by the shear stress of the forward motion, while on the retreating side the directions of the shear stresses are opposite [13]. In this case the material remains longer under the shoulder and the strains are therefore higher [16]. The above-mentioned factors and the extrusion process propelling the material, after plastic deformation occurred, in the TS of the weld, may be responsible for the presence of folds within the TS of the nugget. The stirring action of the threaded probe and the transverse motion along the welding direction [13], appear to be responsible for the formation of bands within the nugget. Strain maps investigations have demonstrated that the strain contours around the probe is similar to the onion ring structure of the nugget [16]. In this case the bands present within the nugget become wider toward the center of the nugget, probably indicating an increase in the strain close to the rotating probe. Within the steady-state weld region, which represents the main weld length, a small equiaxed microstructure is formed. In this latter region a long and high temperature transient is present. In the steady-state weld region, the thermal transient also influences areas beside the weld nugget with subgrain formation and the coarsening of the intragranular precipitates as well as the grain boundary phases [8]. The investigations carried out in the final weld region do not allow to clearly discriminate between rotational, transitional zone and parent material as it was done in experiments with a “frozen” probe [12]. Nonetheless, it is interesting to note how deformation and recrystallization are both present on a layer close to the “rotational zone” (Fig. 8 (a)). Away from this zone (0.5 mm) on a vertical layer closer to the reader, the microstructure exhibits a recrystallized microstructure with small grains but no particular deformation features (Fig. 8 (b)). In the TS, within regions close to “rotational zone”, a slight variation in the grain dimensions is present. The dimension of the grains as well as the longitudinal, vertical and lateral forces also depends on the welding parameters [7], [9], and a slight temperature transient may influence the shape and the dimension of the recrystallized grains. Nonetheless, the grains in the final weld region close to the rotational zone, are generally not equiaxed as observed for instance for the weld nugget in the steady state welding condition. For grains in equilibrium, an equiaxed grain 120° angle grain boundary geometry is generally present [15] and this grain geometry is present at least 1 mm away from the rotational zone. Although within the rotational zone a continuous dynamic recrystallization process takes place [17], forming the microstructure with small grains (Fig. 8), the formation of the typical equiaxed microstructure of the nugget grains takes place with a limited grain growth under static conditions (Fig. 5 (d)) as a crystallization front away from the rotational zone after the probe passes. The temperature in the weld zone remains high for several minutes and gradually decreases as for the pulling out period [6], so that, as observed by other authors [17], static events and limited grain growth

Open Science Index, Mechanical and Materials Engineering Vol:15, No:2, 2021 publications.waset.org/10011823.pdf

due to the adiabatic heat generation [9] may easily occur. A grain growth and the introduction of dislocations are also observed after the rotating tool passes and the extent of the thermal-mechanical deformation is decreased [11]. In this concern, the protraction of an increased temperature level also appears to contribute to the almost complete resolutionizing of the intragranular precipitates within the nugget grains [3]. On the surface beneath the shoulder, the temperature increase also allows the formation of a recrystallized microstructure with small grains (Fig. 7), but the likely rapid temperature decrease after the shoulder passes, limits the grain growth and the extent of the equiaxed microstructure.

V. Conclusions

In regions where the plates are not completely welded and in the final weld region, the deformation and the crystallization processes taking place during the welding can also be observed by means of optical microscopy (a relatively simple investigation technique).

The microstructure exhibits the presence of shear movements along the horizontal plane superimposed by vertical shear movements. The vertical shear can be of opposite directions within very narrow regions, in particular along the plate margin, and is not homogeneous through the plate thickness.

After the probe passes, a grain growth under static conditions may take place. A small grain microstructure, formed directly after a continuous dynamic recrystallization process, becomes a small equiaxed microstructure (nugget).

A material transport influenced by the rotating shoulder has been observed from the trailing to the AS of the weld.

Acknowledgments

The author would like to thank K. V. Jata from the AFRL/ML, WPAFB, R. G. Buchheit, from the Ohio State University and A. P. Reynolds from the University of South Carolina for the welding.

References

[1] Thomas, W.M. et al., Friction Stir Butt Welding, 1991, 1995, GB, U.S.
[2] Nowak, B.M., A.C. Hall and G.A. Knorovsky, High-Speed Video Flow Visualization in Friction Stir Welds of Polycarbonate, The 6th International Trends in Welding Research, Pine Mountain, Georgia USA, 15-19 April 2002, p. 224.
[3] Rhodes, C. G., M. W. Mahoney, W.H. Bingel, R.H. Spurling and C.C. Bampton, Scripta Materilia, 1997, 36, 69.
[4] Askari, A. et al., Modeling and Analysis of Friction Stir Welding Process. Friction Stir Welding and Processing, edited by K.V. Jata. M. Mahoney et al., TMS, 2001.
[5] Frigaard Ø, Grong Ø and O.T. Midling, A Process Model for Friction Stir Welding of Age Hardening Aluminum Alloys, Metall. Mater. Trans. A, May 2001, 32 A, pp. 1189-1200.
[6] Song M. and R. Kovacevic, Numerical and Experimental Study of the Heat Transfer Process in Friction Stir Welding, J. Engineering Manufacture, Proc. Instn. Mech. Engrs., Vol 217, Part B, pp. 73-85, 2003
[7] Chen C. and R. Kovacevic, Thermo-mechanical Modelling and Force Analysis of Friction Stir Welding by the Finite Element Method, J. Mechanical Engineering Science, Proc. Instn. Mech. Engrs., Vol 218, Part C, pp. 509-519, 2004.
[8] Mahoney, M.W. C.G. Rhodes, J. G. Flintoff, R.A. Spurling and W. H. Bingel, Properties of Friction-Stir-Welded 7075 T651 Aluminum, Met. Trans. A 29, 1998, pp. 1955-1964.
[9] Murr L.E., Y. Li, R.D. Flores, E.A.Trillo and J.C. McClure, Intercalation Vortices and Related Microstructural Features in the Friction-Stir Welding of Dissimilar Metals, Material Research Innovation, 1998, 2, pp.150-163.
[10] Seidel, T.U. and A.P. Reynolds, Visualization of the Material Flow in AA2195 Friction-Stir Welds Using a Marker Insert Technique, Metallurgical and Materials Transactions A 32, 2001, pp. 2879-2884.
[11] Su J. Q., T. W. Nelson and C. J. Sterling, Microstructure Evolution during FSW/FSP of High Strength Aluminum Alloys, Materials Science and Engineering A 405, pp. 277-286, 2005.
[12] Guerra, M., et al., Metal Flow during Friction Stir Welding, in Friction Stir Welding and Processing, K. V. Jata, R. S. Mishra, S. L. Semiatin, D. P. Field, Editor, 2001, TMS Indianapolis, Indiana, p. 246.
[13] Ouyang J.H., D. Jandric, R. Kovacevic, M. Song and M. Valant, Visualization of Material Flow during Friction Stir Welding of the Same and Dissimilar Aluminum Alloys, Trends in Welding Research, Proceedings of the 6th International Conference, Pine Mountain, Georgia, 2002, pp. 229-234.
[14] Jata, K.V. and S.L. Semiatin, Continuos Dynamic Recrystallization During Friction Stir Welding of High Strength Aluminum Alloys, Scripta Materialia 43, 2000, pp. 743-749.
[15] Honeycombe, R.W.K., Normal Grain Growth, The Plastic Deformation of Metals, Section 11.12, p. 319, E. Arnold, Editor, 1984, ASM, U.K. p. 483.
[16] Heurtier P., C. Desrayaud and F. Montheillet, A Thermomechanical Analysis of the Friction Stir Welding Process, ICAA 8, Cambridge U. K., 2-5 July 2002, pp. 1537-1542.
[17] Li Y., L.E. Murr and J.C. McClure, Flow Visualization and Residual Microstructures Associated with the Friction-Stir Welding of 2024 Aluminum to 6061 Aluminum, Materials Science and Engineering A 271, 1999, p. 213-223.
[18] Cingara G.A., H. J. McQuenn, A. Hopkins, V. Jain and D.D. Perovic, Light Weight Al Alloys for Aerospace Applications, ed. E.W. Lee, N.J. Kim, K.V. Jata and W.E. Frazier, 1995.